Catalysis Today 157 (2010) 24–32

Contents lists available at ScienceDirect

Catalysis Today

journal homepage: www.elsevier.com/locate/cattod

Multiscale process intensification for catalytic partial oxidation of methane: From nanostructured catalysts to integrated reactor concepts

Götz Veser[a,b]

[a] Chemical Engineering Department, Swanson School of Engineering, 1249 Benedum Hall, University of Pittsburgh, Pittsburgh, PA 1561, USA
[b] U.S. Department of Energy, National Energy Technology Laboratory, 626 Cochrans Mill Road Pittsburgh, PA 15236, USA

ARTICLE INFO

Article history:
Available online 9 June 2010

Keywords:
Process intensification
Catalytic partial oxidation
Methane
Syngas
Integrated reactors
Nanocatalysts

ABSTRACT

Process intensification (PI) is an exciting area of chemical and process engineering with increasing importance in the design and development of cleaner, more efficient, and more sustainable processes. The present contribution reviews work from the author's laboratory on catalytic partial oxidation of methane (CPOM) as example for a multiscale approach to process intensification. It is shown that regenerative heat-integration via flow reversal is an efficient way to overcome thermodynamic limitations present at autothermal reactor operation, and that "nano-engineered" catalysts can complement and enable these reactor concepts by combining high activity with exceptional catalyst stability. Most significantly, the combination of heat-integration with nanostructured catalysts yields synergies which are characteristic for multiscale process intensification, resulting in the present case in strongly increased syngas yields of 80% in a simple, air-fed autothermal CPOM process.

1. Introduction

The foreseeable end of fossil energy resources combined with the rapid industrialization of the developing world and the unsustainable level of anthropogenic greenhouse gas emissions have resulted in an accelerating push for new ways of providing the energy for our modern way of life. However, the range of recommendations and predictions of future energy production diverges strongly: while some scenarios require a transition to direct solar energy as the dominant, or even sole, energy source, others predict that a broad technology mix of nuclear energy, biofuels, wind and solar energy, and even a (limited) continued use of fossil fuels, will offer a sustainable solution both in economic as well as environmental terms [1]. In view of this transition and the associated uncertainty regarding the long-term economical and political viability of different technologies, the paradigm of the "economy of scale" has become increasingly questionable and is sometimes even regarded as a major hurdle for implementation of novel technologies [2]. For example, biofuels require utilization of comparatively small, distributed resources, rendering large-scale plants uneconomical [3]. Similarly, efficient utilization of small-scale local resources is quickly becoming a necessity for domestic chemical industry to remain competitive in an increasingly globalized market. These trends are motivating the design of small(er)-scale, decentralized processes and plants, which offer multiple advantages, since they cannot only utilize such small-scale distributed resources more efficiently, but can also react much more flexibly to changes in political climate, resource availability, cost, and competition. Furthermore, the reduced cost of building small-scale facilities helps to lower the economic hurdle towards implementing new technologies, and reduces the fear of being "locked in" to technologies for many decades, in particular in view of the uncertainty of political and other frameworks that might render these technologies obsolete or uneconomical.

In chemical process engineering, this development is often summarized by "process intensification", i.e. the development of smaller, safer, more flexible, more efficient, and less costly processes based on the utilization of novel equipment and devices, and through the development of novel technologies and methodologies. The present contribution aims to illustrate this approach by giving a review of results on catalytic partial oxidation of methane to synthesis gas from the author's laboratory. A particular emphasis is put on the often neglected aspect of multiscale engineering in process intensification, i.e. on an approach in which the application of reactor-scale measures (here: the utilization of a heat-integrated reactor concept) is combined with the simultaneous development of catalyst- or reactant-level measures (here: nanostructured catalysts) in a way that results in strong synergies.

2. Process intensification—definition and tools

Process intensification ("PI") is still a fairly young area and correspondingly no broadly accepted definition of this term exists

E-mail address: gveser@pitt.edu.

0920-5861/$ – see front matter © 2010 Elsevier B.V. All rights reserved.
doi:10.1016/j.cattod.2010.04.040

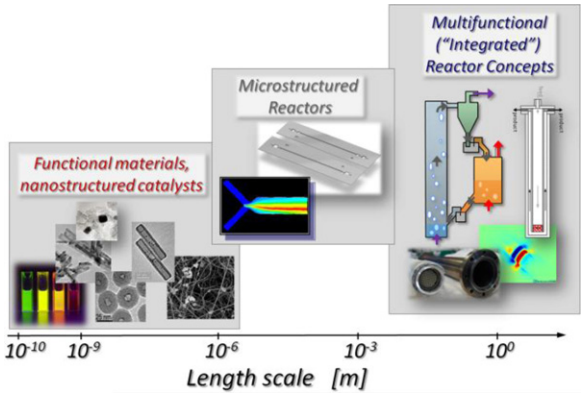

Fig. 1. Multiscale reaction engineering toolbox for process intensification, ranging from nanostructured materials, over microchemical reactors, to fully integrated, multifunctional reactor concepts.

to-date. The term "process intensification" is usually attributed to Ramshaw who defined it in the mid-1980 as the development of new processes with a substantial reduction in plant size by "at least a factor of 100" [4]. The reduction of plant size results in substantial cost reduction and improved reactor safety due to better control over reaction conditions and reduced inventory and hold-up of chemicals. Due to this early definition, process intensification is often reduced to the development of microchemical reactors ("microreactors") and other "microprocess equipment", which is unique in indeed offering the potential of reducing reactor size by orders of magnitude. However, such drastic size reduction may be overly ambitious and restrictive for industrial practice, and a more recent definition from the "European Road Map for Process Intensification" hence defines PI much more broadly as "a set of often radically innovative principles ("paradigm shift") in process and equipment design, which can bring significant (more than factor 2) benefits in terms of process and chain efficiency, capital and operating expenses, quality, wastes, process safety, etc.' [5,6]. It is noteworthy that this definition does not explicitly mention size at all anymore, but rather focuses on the effect of the "innovative principles" on various aspects of process efficiency, i.e. it focuses on the outcome rather than the means of these process improvements.

Specifically, this more recent definition lends itself to taking full advantage of the multiscale nature of catalytic processes, which leads naturally to a broadening of the toolbox for PI engineering (see Fig. 1): in addition to "microprocess engineering" [6–8], which allows in particular optimization of heat and mass transport processes, characterized by length scales in the micrometer to millimeter range, strong improvements can be achieved from integration of multiple unit operations into a integrated, or "multifunctional" reactor on the macroscale, as well as from harvesting the emerging potential of functional materials on the nanoscale. Process intensification is thus becoming a true multiscale endeavour which integrates novel materials (nanomaterials), novel equipment (microprocess equipment), and novel methodologies (multifunctional reactors).

Multifunctional reactors have already developed into an area of very active research [9–11], although the label "multifunctional" is more aspirational than factual as virtually all concepts that have been realized to-date are of the "reaction plus one" type, i.e. they are bi- rather than multifunctional and "integrate" the reaction with one additional unit operation. The most investigated concepts to-date are:

- *Reaction plus separation*: these concepts are usually used to break equilibrium limitations or avoid further reactions of desired intermediates by withdrawal of the respective reaction product. Examples include reactive distillation [12], membrane reactors [13], or chromatographic reactors [14], where in particular the first has already found some impressive industrial application [15].
- *Reaction plus mixing*: examples here include the spinning disk reactor [16,17], where an artificial force field is imposed in order to achieve more intense mixing, and membrane reactors in which the membrane is utilized to achieve a distributed reactant feed. Targets are typically increased conversion and/or selectivity in the first case, and increased process safety in the second case (by avoiding the mixing of potentially flammable or explosive mixtures), although selectivity improvements can occasionally also be the target.
- *Reaction plus heat-exchange*: in this case, heat-exchange is integrated directly into the reactor, either via regenerative or recuperative heat-exchange, with the aim to increase the energy efficiency of a process, extend the limits of autothermal reactor operation, or break (autothermal) thermodynamic limitations [18,19].

Illustration of these principles is well beyond the scope of the present article, and the reader is referred to a number of recent monographs for more detailed information [20–22]. The present article will restrict itself to using results from the author's laboratory to illustrate the "reaction plus heat-exchange" principle via application of a heat-integrated reactor concept to syngas production from methane.

Beyond the above mentioned two reactor engineering-based principles of PI, a new area for process intensification is emerging with the dramatic advances in nanotechnology, specifically the control of catalyst properties on the nanometer and sub-nanometer scale. While changes in catalyst are often explicitly excluded from definitions of process intensification in order to avoid confusion with entirely new reaction pathways and/or new process chemistries, we consider "nano-engineering" of catalysts – i.e. using nanostructuring to affect catalyst properties without changing the chemical composition of the catalyst – an exciting emerging area which needs to be included in the PI toolbox in order to fully harvest the potential of a true multiscale "intensification" of chemical processes. Again this article will use selected results from the author's laboratory on the development of novel catalysts for CPOM to illustrate how nanomaterials can complement and enable reactor engineering approaches towards intensified processes, and how the combination of these multiscale measures can result in strong synergies for the resulting process.

3. Application: hydrogen and syngas from methane

Conversion of methane to syngas and/or hydrogen has been the focus of much research and development over the past two decades [23,24]. At present, the main industrial route for the production of syngas is steam reforming of methane (SRM):

$$CH_4 + H_2O \rightarrow CO + 3H_2 \qquad \Delta H_R = +206\,kJ/mol$$

SRM is a highly endothermic process which requires a large amount of energy, typically supplied via methane combustion in externally fired tubular reformers. This results not only in significant emissions of CO_2 from SRM, but also limits its overall thermal efficiency, in particular for small-scale, decentralized processes [25].

Autothermal reforming of methane (ATR) is an alternative to SRM which avoids these limitations [24,26]. In ATR, methane combustion is directly integrated with the steam reforming reaction inside the tubular reformer by adding oxygen to the reactor feed in order to couple the endothermal steam reforming with the highly

exothermal combustion of methane.

$$CH_4 + 2O_2 \rightarrow CO_2 + 2H_2O \qquad \Delta H_R = -802\,kJ/mol$$

The resulting process is energetically quite efficient, but it requires a fairly complex redesign of the reactor in which a burner is placed in front of a homogeneous reaction zone followed by a single catalyst bed. Hence, ATM technology is rather expensive and does not lend itself easily to adaptation for small-scale processes.

Catalytic partial oxidation of methane (CPOM) is a third alternative for synthesis gas production, which has emerged as a strong candidate for small-scale processes in recent years [27–29]. The most attractive features of CPOM are the extremely high reaction rates, which allow residence times in the millisecond range, and the mildly exothermicity of the reaction, which allows autothermal operation:

$$CH_4 + 1/2O_2 \rightarrow CO + 2H_2 \qquad \Delta H_R = -37\,kJ/mol$$

Furthermore, in contrast to non-catalytic partial oxidation processes, the very high reaction rates of CPOM allow operation of the process at comparatively mild temperatures (~1000 °C) and hence open up the possibility of an air-blown process without significant NO_x problems. This makes this reaction route particularly attractive for small-scale decentralized processes: the reaction can be conducted in simple, single-pass tubular flow reactors with extremely high space-time yields and hence highly compact reactors. However, a thermodynamic analysis shows that the adiabatic temperature rise for the partial oxidation of a stoichiometric methane/air mixture is only about $\Delta T_{ad} \sim 250$ °C, well below the temperatures which are thermodynamically required for optimal syngas yields (>900 °C). The temperatures in excess of 1000 °C which are experimentally observed in this reaction are therefore not due to the partial oxidation reaction itself, but rather due to combustion of some of the methane feed. The reaction yield is thus determined by a complex interplay between partial and total oxidation reactions [30,31]: the combustion of methane results in high temperatures which shift the reaction equilibrium towards the partial oxidation route. At the same time, however, this formation of total oxidation products also results in reduced syngas selectivity. Overall, this interplay thus limits attainable synthesis gas yields at autothermal operation.

3.1. Heat-integrated reactors

The above discussed autothermal limitation in methane partial oxidation constitutes a classical example for the application of heat-integrated reactors: in such reactors the catalytic reaction is coupled with an internal heat-exchange between the hot product gases and the cold feed gases, resulting in a highly efficient use of the mild exothermicity of the partial oxidation reaction [19,32]. This internal heat-exchange can be achieved in a very straightforward way via recuperative heat-exchange in a counter-current heat-exchange reactor [33,34]. A somewhat more complex, yet more efficient way of heat-integration is the regenerative heat-integration via periodic flow reversal [35–37]. The principle of this reactor concept is illustrated in Fig. 2: the top panel shows the catalytic reactor in which a catalyst is surrounded by inert zones and the flow direction can be switched via three-way valves on either end of the reactor; the bottom panel shows the development of the temperature profile through the reactor during one flow reversal: initially, the reactor feed enters the reactor via 'F_1', i.e. reactants flow through the reactor from left to right. Upon entering the catalyst zone, the reaction occurs and the heat of reaction is released, raising the temperature of the catalyst, of the product gases, and thus of the downstream inert zone. At reverse-flow operation, the gas flow through the reactor is reversed at a certain time so that

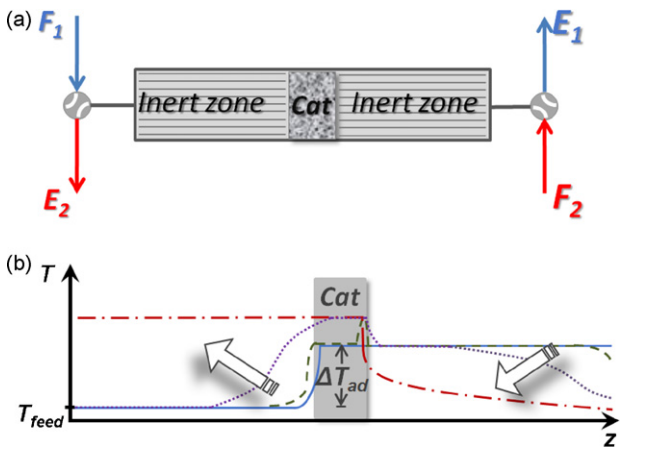

Fig. 2. (a) Reactor concept of a reverse-flow reactor and (b) corresponding schematic temperature profiles through the reactor upon one flow reversal (gases flowing from right to left, corresponding to schematic valve position in (a)).

cold feed gases are now entering via 'F_2' and get pre-heated by exchanging heat with the hot inert zone. The reactants thus hit the catalyst at already elevated temperature which is then further raised via release of the heat of reaction. When exiting the catalyst zone, the hot product gases now exchange heat with the downstream inert zone, cooling down the gases and heating up this inert zone. Upon the next flow reversal, this cooling–heating cycle is repeated again, this time in the opposite direction. If this flow reversal is repeated at an appropriate cycling frequency, a so-called "periodic steady-state" is eventually reached which is characterized by temperature and concentration profiles which are mirror images of each other during two subsequent half-periods. Overall, this concept hence results in two very advantageous thermal characteristics: it is possible to attain super-adiabatic temperatures in the reaction zone without any additional external heat supply, while both reactor ends and the effluent gas stream remain at comparatively mild temperatures, reducing the materials demands on the reactor periphery in high-temperature reactions significantly.

The effect of this efficient heat-integration is shown exemplarily in Fig. 3 [38]: Fig. 3a (left) shows experimentally measured temperature profiles during reverse-flow operation of catalytic partial oxidation of a stoichiometric mix of methane with air over four half-cycles in the catalyst zone (z = 0–10 mm) and in one of the two inert zones (z = 10–40 mm) after attaining the periodic steady-state. One can see how the flow switching results in an almost instantaneous jump of the reaction front inside the catalyst zone from one end to the opposite end of the catalyst (see location of the dark red maxima in the temperature profile), while the temperature in the inert zone is reacting comparatively slowly to the changes in flow conditions. The reactor temperatures in the catalyst zone are about 1000 °C, i.e. well above the adiabatic temperature rise, while the temperature at the end of the inert zone remains comparatively cold, demonstrating efficient heat integration.

As a result, the syngas yields during reverse-flow operation of the reactor are strongly increased in comparison to conventional, steady-state reactor operation: Fig. 3b shows strong improvements in CO and H_2 yields when reactor operation is changed from steady-state (open symbols) to reverse-flow (filled symbols). These improvements are particularly pronounced at high flow rates: while syngas yields show a maximum around 3 slm at steady-state operation, they increase continuously all the way up to 9 slm (which constitutes the limit of the experimental set-up) during RFR operation. This again reflects the nature of the heat-integration: at steady-state operation, increasing flow rates eventually result in a convective cooling of the catalyst, pushing the reaction front fur-

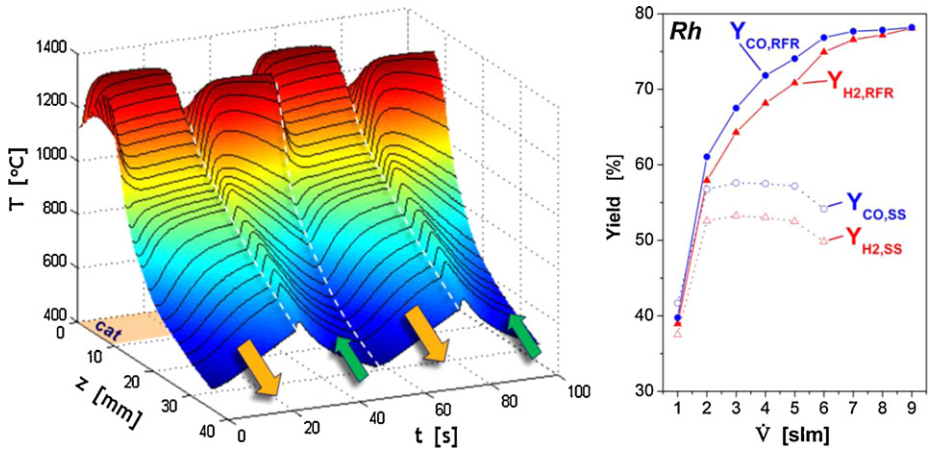

Fig. 3. (a) Typical temperature profiles in the catalyst (z = 0–10 mm) and one inert zone over four subsequent half-cycles during reverse-flow operation. (b) Syngas yields vs. volumetric feed gas flow rate for an Rh/Al_2O_3 catalyst. CO (squares) and H_2 yields (circles) for a conventional 'steady-state' reactor (SS, open symbols and dotted lines) are shown in comparison with results in a reverse-flow reactor (RFR, filled symbols and solid lines). Conditions: stoichiometric feed of CH_4/air, RFR periodicity: 25 s, total feed flow rate (left graph): 2 slm.

ther into the catalyst, and hence reducing the effectively usable catalyst length. Heat-integration avoids this effect by internally pre-heating the cold feed gases. Hence, the catalyst cooling is avoided and the full catalyst length remains available for the catalytic reaction. Additionally, the increasing heat generation with increasing flow rate results in hotter inert zones and hence further improves the heat-integration, i.e. it results in further increased pre-heating and hence further improved syngas yields. The regenerative heat-integration thus allows much higher through-puts than steady-state operation without loss of yield, making this concept particularly well-suited for compact reactors and distributed processes.

However, the detailed design of integrated, multifunctional reactors requires careful consideration of other effects of the integration of multiple unit operations into one apparatus, since the interplay between these unit operations can have effects beyond the intended ones. For heat-integrated reactors, for example, the effect of the strong pre-heating on possible pre-catalytic gas-phase reactions needs to be considered, since these must usually be avoided due to selectivity losses and safety concerns [39,40]. This is of particular concern for fuel processing, where potentially flammable or even explosive mixtures of fuels and oxidizing gases need to be handled. However, the availability of fairly robust and reliable homogeneous reaction kinetics for many of these systems allows calculation of reactor operating envelopes within which safe and efficient operation is possible [39,40].

Another issue in the development of PI concepts regards the quantification of the 'intensification' or efficiency of the integration which is achieved with these novel reactor concepts. Process intensification can have many different, specific targets (as discussed in Section 1) – such as increased space-time yield, waste minimization, reduced reactor size or cost, improved efficiency of product separation, reduced overall process operating cost – and it is necessary to define clearly quantifiable measures to capture the efficiency or degree of the respective "intensification". For heat-integrated reactors, we have previously proposed a straightforward measure of efficiency [32]. The concept is illustrated in Fig. 4a which shows schematically the (standard) enthalpy of a reactor effluent from a conventional reactor and a heat-integrated reactor. The enthalpy, $H(T) = H^\theta + C_p \Delta T$, can be separated into the "latent heat", H^θ, and the "sensible heat", i.e. $C_p \Delta T$ (where $\Delta T = T - T^\theta$). In the conventional process, the effluent leaves the catalyst at relatively high-temperature ($T_{exit,SS}$) and relatively low standard enthalpy (H^θ_{SS}), i.e. low selectivity. In comparison, heat-integration results in a lowering of the effluent temperature ($T_{exit,RFR}$) and an increase in enthalpy (H^θ_{RFR}) due to increased reaction yields, as seen above. The difference between the two effluent temperatures, $T_{exit,SS}$ and $T_{exit,RFR}$, represents the amount of sensible heat which is available for heat-integration (represented by the horizontal line in Fig. 4), which can be calculated from:

$$\dot{H}_{sh} = \sum_i \dot{n}_{i,SS} \cdot (c_{p,i} T_{exit,SS} - c_{p,i} T_{exit,RFR})$$

where $\dot{H}_{sh}$ is the flow of sensible heat, $\dot{n}_{i,SS}$ is the molar flow of component i, $c_{p,i}$ the heat capacity of species i, $T_{exit,SS}$ the catalyst exit temperature in the conventional ("steady-state") process, and $T_{exit,RFR}$ the reactor exit temperature in the heat-integrated ("RFR") process. $\dot{H}_{sh}$ thus represents the maximum amount of heat per unit time which is available for heat-integration.

On the other hand, the difference between the enthalpies of the conventional and the heat-integrated process at temperature $T_{exit,RFR}$ (the vertical line in Fig. 4) is equal to the difference in latent heat of the product gases (i.e. the difference in chemical energy). It is calculated with the respective product gas compositions at the exit temperature of the heat-integrated reactor as:

$$\Delta\dot{H}_{RFR-SS} = \sum_i \dot{n}_{i,RFR} H_i(T_{exit,RFR}) - \sum_i \dot{n}_{i,SS} H_i(T_{exit,RFR})$$

The heat-integration hence results in a conversion of sensible heat into latent heat or 'chemical energy', the efficiency of which can now be calculated as a ratio of the two heat flows:

$$\eta = \frac{\Delta\dot{H}_{RFR-SS}}{\dot{H}_{sh}}$$

Using this definition, Fig. 4b shows the calculated the efficiency of the RFR concept as a function of flow rate for a stoichiometric methane/air mixture [38]. The strong increase in efficiency with increasing flow rate again emphasizes that the heat-integrated reactor concept is particularly well-suited for small-scale, compact reactors with high-throughput, as already seen above in the increasing syngas yields with increasing flow rate (cp Fig. 3b).

3.2. Heat-integration and catalyst stability

The above discussed results demonstrate the efficiency of a heat-integrated reactor concept for high-temperature fuel processing. However, the discussion has so far neglected a key concern in

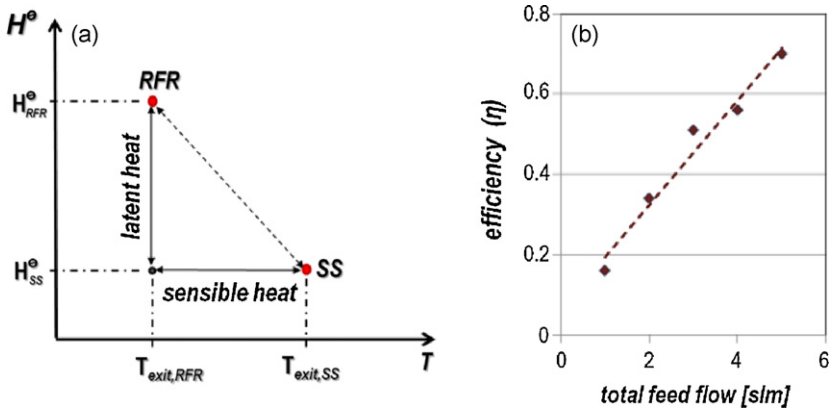

Fig. 4. Quantifying "process intensification". (a) Schematic diagram of standard enthalpy H^{θ} vs. temperature, illustrating the conversion of sensible heat into latent heat in a heat-integrated reactor. (b) Calculated efficiency of heat-integration for a stoichiometric mix of methane/air in a tubular reactor at reverse-flow vs. steady-state operation.

high-temperature catalysis, namely catalyst stability [41]. Catalyst stability is a significant concern in virtually all industrial catalytic processes, and this concern is strongly exacerbated by the high temperatures characteristic for short contact-time fuel processing applications since most catalysts show rapid deactivation at temperatures in excess of ~600–800 °C. Based on the above discussion of heat-integrated reactors, one can expect that the increased reactor temperatures and continuous temperature oscillations inside the catalyst zone, which characterize RFR operation, result in accelerated catalyst deactivation.

Surprisingly, a cursory look at experimental results seems to suggest that catalyst stability is in fact unaffected by the periodic reactor operation: Fig. 5a shows the hydrogen selectivity for CPOM over a Pt-based catalyst [42], where open diamonds show results at RFR operation and filled squares show results from SS operation of the same reactor. As seen above, RFR operation results in strongly improved hydrogen selectivity, but, counter to expectations, catalyst deactivation is comparable in both reactor operation modes, with a decrease from ~91% to 82% at RFR and from ~75% to 68% at SS operation, i.e. about 10% decrease in both cases. A closer look, however, reveals that the true catalyst deactivation is indeed strongly accelerated at RFR conditions: when temporarily switching off the periodic flow reversal during RFR operation and allowing the system to attain a steady-state, one observes a strongly exacerbated catalyst deactivation, as shown by the filled diamonds in Fig. 5a. Clearly, the catalyst does deactivate much more rapidly at the elevated temperatures and demanding conditions of RFR operation—but the heat-integration in the RFR reactor compensates virtually entirely for this deactivation! It is a well-established procedure in the industrial practice of catalytic reactor operation to increase reactor temperatures in order to (temporarily) compensate for catalyst deactivation. Unlike this deliberate control measure in a conventional reactor, the heat-integrated reactor is self-compensating: catalyst deactivation results in increasingly unselective (total) oxidation, and hence in increasing heat release. The RFR immediately re-integrates this additional heat into the reaction zone via the above described regenerative heat-exchange, hence intrinsically adjusting to the worsening performance of the catalyst. This self-adjusting characteristic again makes the reactor concept highly attractive for decentralized processes, where continuous monitoring capabilities and the availability of operating personnel might be limited.

This interesting phenomenon has further implications which can be seen when comparing the performance of different catalysts in CPOM: Fig. 5b shows again hydrogen selectivities for four metals commonly used in partial oxidation catalysis (Pt, Rh, Ir, Ni) [42]. One can see that at SS operation strong differences exist in the performance between these metals (up to 35% difference), with

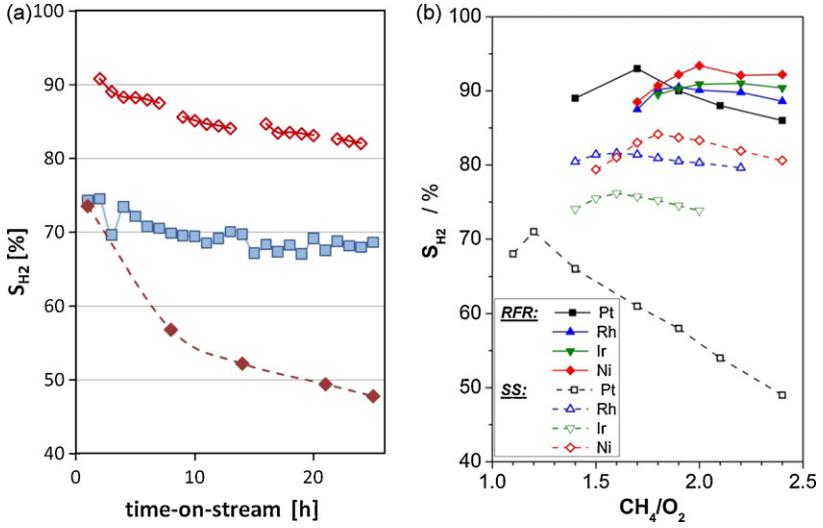

Fig. 5. Effect of heat-integration on catalyst performance and stability. (a) H_2 selectivity as function of time for a Pt-based catalyst at reverse-flow reactor (RFR) operation (top line, open diamonds), conventional steady-state (SS) reactor operation (middle line, filled squares), and for steady-state measurements in-between reverse-flow operation. (b) H_2 selectivity for several different catalysts vs. methane/oxygen ratio at RFR and SS operation. Total feed flow is 3 slm, and RFR periodicity is 15 s.

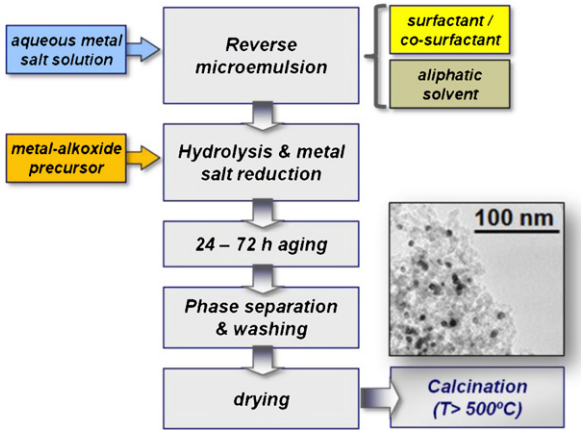

Fig. 6. Synthesis pathway for nanostructured high-temperature catalyst via a reverse-microemulsion templated sol–gel process. The TEM image shows a typical catalyst material.

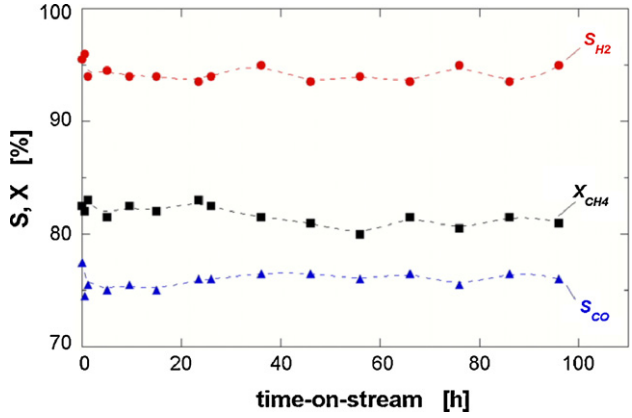

Fig. 7. Methane conversion, CO selectivity, and H_2 selectivity during catalytic partial oxidation of methane with air (=1.7) over a nanostructured Pt-BHA catalyst vs. time. Operation is in a conventional steady-state flow-tube reactor with a total feed flow rate of 3 slm. Selectivity is calculated as $S_{H_2} = 2 \times F_{H_2,out}/(F_{CH_4,in} - F_{CH_4,out})$ and $S_{CO} = F_{CO,out}/(F_{CH_4,in} - F_{CH_4,out})$.

Pt showing the lowest hydrogen selectivities and Ni and Rh the best. However, at RFR operation, all four catalysts show very similar performance (within <10%). The heat-integration hence not only compensates for a deactivating catalyst, as seen above, but also compensates for the poor performance of intrinsically less selective catalysts by re-integrating the strong heat release from unselective total oxidation and hence improving overall syngas yields. This suggests that catalyst robustness might ultimately be the more critical catalyst development target for this reaction system than selectivity, since the reactor concept can efficiently compensate for the lack of the latter, but only temporarily "bridge" the decaying activity of a deactivating catalyst.

3.3. Nano-engineered catalysts

The results from the reactor studies discussed above suggest that – not surprisingly – heat-integrated reactor systems require particularly robust catalyst systems. This demand for new, "tailored" catalysts may in fact apply to many intensified processes and integrated reactor concepts: microreactors typically require the development of new catalyst coating techniques or at least the fine adjustment of existing techniques to the demands of the new materials and dimensions of micromachined units, and membrane reactors for dehydrogenation reactions and/or hydrogen production, for example, are notorious for the occurrence of drastic catalyst coking issues due to the hydrogen removal. It is hence desirable – if not necessary – to develop PI reactor concepts in conjunction with suitable catalysts systems, and, as mentioned in Section 1, the artificial distinction between the more "engineering-oriented" process intensification and the more "chemist-dominated" catalyst development is, at best, not helpful.

In this context, the emergence of "nano-synthesis" pathways over the past two decades is beginning to offer an unprecedented degree of control over catalyst properties from the nanoscale up [43]. While the prediction of selectivity changes with catalyst size is still largely impossible at this point in time, "nanoscaling" the active component of a catalyst can be expected to result in increased activity due to the strong increase in active surface area, if not due to true nanoscale phenomena [44]. However, with decreasing particle size the stability of materials is typically compromised due to the well-established melting-point depression for nanomaterials which leads to strongly increased sintering [45,46]. Despite the vast amount of work in the area of nanocatalysis over recent decades and the obvious importance of this aspect for the application of nanomaterials as technical catalysts, this lack of stability of nanomaterials has found surprisingly little attention to-date.

In order to overcome the stability limits of nanoscaled catalysts in the present case, we developed a pathway to nanostructure both the active metal as well as the ceramic support in order to stabilize the metal nanoparticles via a robust embedding into the ceramic matrix [47,48]. The synthesis is based on a reverse-microemulsion templated sol–gel synthesis of nanometer-sized catalyst particles [49,50]. We limit the brief discussion here to platinum as the active component of the catalyst – although extension onto a broad range of metals [51–53], including metal alloys [54], is fairly straightforward – and to a high-temperature stabilized alumina support (barium hexaaluminate, BHA), a material which was developed originally by Arai and Fukuzawa for high-temperature combustion applications and is hence well-suited for high-temperature catalysis [55].

The steps in the catalyst synthesis are summarized in Fig. 6. A reverse-microemulsion is formed by combining an aqueous metal salt solution (here: hexachloro-platinic acid), an aliphatic solvent (such as iso-octane), and one of a range of commercially available non-ionic surfactants. Then, a stoichiometric mixture of the oxide precursors (here: Al- and Ba-alkoxides) is slowly added to the microemulsion, starting the hydrolysis reaction. After aging and thermally-induced phase separation, the resulting gel is washed several times, vacuum-dried, and finally calcined at temperatures above 500 °C to remove any residual surfactant and carbonaceous deposits. The resulting powders are loosely agglomerated nanocomposites of homogeneously distributed metal particles in a hexaaluminate matrix and were typically used as synthesized. Due to the controlled nanostructure with a highly interconnected mesopore network the materials not only show very high specific surface areas (in excess of 100 m^2/g after calcinations at temperatures as high as 1000 °C) but also allow easy access to the active component, which is a critical aspect in order to avoid mass transfer limitations at the very high reaction rates of high-temperature catalysis.

Fig. 7 shows a typical result of the performance of these catalysts in CPOM in a conventional, steady-state flow-tube reactor [56]: one can see that not only the syngas selectivity and methane conversion are significantly improved in comparison to the performance of a conventional catalyst, but the catalyst performs without any signs of deactivation over the entire duration of the experiment (~100 h) while the conventional catalyst showed significant deactivation even after ~20 h operation (compare to the SS curve in Fig. 5a). Clearly, nanostructuring the catalyst resulted not only in a highly active, but also in an exceptionally stable catalyst.

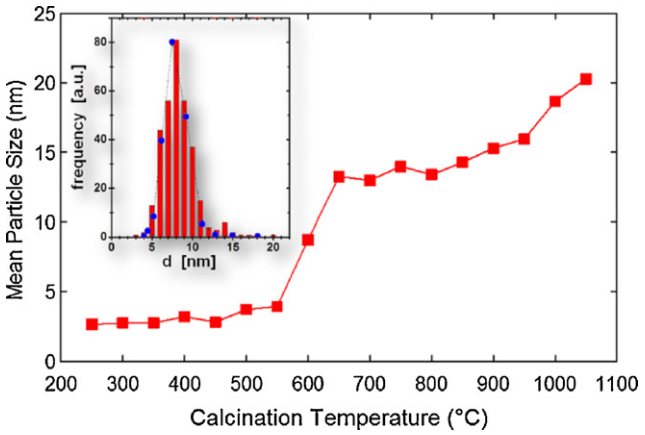

Fig. 8. Pt particle size as a function of calcination temperature. The inset shows Pt particle size distribution (determined from TEM images, red bars) and BHA pore size distribution (calculated from BJH evaluation of N_2 sorption experiments, blue dots) after calcination at 600 °C. The duration of the calcination was in each case 2 h. (For interpretation of the references to color in this figure legend, the reader is referred to the web version of the article.)

This stability can indeed be traced back to the embedding of the Pt nanoparticles in the mesopore structure of the hexaaluminate. Fig. 8 shows the development of the Pt particle size vs. calcination temperature, as determined from TEM measurements. The nanoparticles are initially very small (<5 nm) up to calcination temperatures of ~500 °C. Above this temperature, the nanoparticles become sufficiently mobile that particle growth occurs. However, surprisingly, the sintering process stops at ~14 nm average particle size, and the particle remain essentially stable at this size up to temperatures above 900 °C. (Further experiments confirmed that the particles remain indeed stable at this size for extended duration of the calcinations up to at least 20 h.)

The inset shows the statistical particle size distribution (from TEM, bars) along with the pore neck size distribution of the same material (from a BJH analysis of the desorption branch of a N_2 sorption experiment, dots) after calcination at 600 °C [57]. One can see that there is virtually perfect agreement between the two size distributions, suggesting that the particle size is determined by the size of the pore necks. This confirms the original concept in stabilizing the metal nanoparticles: when the calcination temperature (or the reaction temperature) becomes sufficiently high, the metal nanoparticles start to migrate and agglomerate, resulting in sintering of the active component in the catalyst. However, this sintering is stopped once the particles grow beyond a certain size, since they do not fit through the relatively narrow pore necks anymore and their mobility is hence restricted. This stabilization remains functional until, with further increasing temperature, the pore structure of the oxide matrix starts to soften and/or collapse, or until the metal nanoparticles start to melt and are hence not restricted by the rigid pore structure any more. Since this stabilization is based on a purely mechanical 'caging' of the particles and is hence independent on the nature of the metal nanoparticle or on specific metal–support interactions, it is applicable to a wide range of metals and support materials.

Beyond stability, an additional concern in utilizing these catalysts in a technical reactor environment is the final catalyst formulation: while in our simple laboratory experiments the nanostructured catalysts were used as synthesized, i.e. as fine powders with particles in the micrometer size range, technical application will typically require supporting the nanostructured metal/support system on a "macroscopic" support structure. In particular for the short contact-time, high-throughput conditions that characterize many fuel processing applications, monolithic

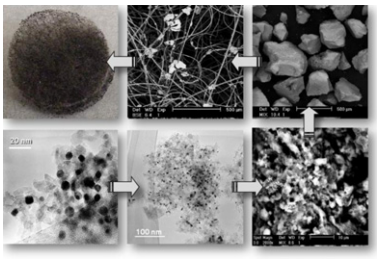

Fig. 9. Pt-BHA coated silica felt catalyst, illustrating the hierarchical structuring of the catalyst across many length scales from the nano- to the macroscale. Counter-clock wise from bottom left: TEM image of Pt nanoparticles embedded in BHA; TEM image of Pt-BHA nanocomposite particle; SEM image of the macropore structure of a nanocomposite particulate; SEM image of particulates, SEM image of Pt-BHA-coated silica fibers; photo of the Pt-BHA coated silica felt catalyst.

structures have found much interest recently due to low pressure drop, relatively high surface areas, and easy handling. Supporting nanostructured catalysts onto such supports without loss of their carefully controlled structure and properties is an area which needs further development as more and more "nanocatalysts" emerge from laboratory studies. For the present catalyst system we have been able to demonstrate supporting the nanostructured Pt-BHA material on different support structures, including monolith and felt structures (Fig. 9), without significant loss in activity or stability, by a simple dip-coating procedure [51]. This demonstrates that such a hierarchical structuring of a technical catalyst from the nanoscale to the macroscale is possible and may in some cases even be achievable with comparatively simple means.

3.4. Combining nanocatalysts and reverse-flow operation

A final test for a true "multiscale process intensification" is the combination of the nanostructured catalyst with the heat-integrated reactor system. Key concern for this multiscale integration is the robustness of the individual process improvements, i.e. that the individual improvements based on the catalyst and the reactor development, respectively, are maintained upon integration, while the combination should additionally yield "synergetic" improvements that exceed the individual advances achieved based on either concept alone.

For the present system, this robustness upon combination of the nanostructured catalyst with the reverse-flow reactor operation mode was confirmed in that the nanostructured catalyst maintained its outstanding stabilility even at the demanding conditions of reverse-flow operation [25]. More importantly, a comparison of results obtained with (a) a conventional Pt/Al_2O_3 catalyst in the RFR, (b) the nanostructured catalyst in a conventional steady-state flow-tube reactor, and (c) the combination of the nanostructured catalyst with the RFR operation shows that the latter combination indeed results in strong synergies (Fig. 10): while the combined concept "inherits" the high CO selectivity from the heat-integrated reactor concept and the excellent H_2 selectivity from the nanocatalyst, it exceeds both significantly in CH_4 conversion. This can be explained by the fact that oxygen is the limiting reactant in this reaction system, so that selectivity improvements result in increased availability of oxygen for further partial oxidation of methane and hence in increased methane conversion. Furthermore, only by combining the nanostructured catalyst with the heat-integrated reactor concept equal selectivity to both syngas components and the desirable ratio of $CO:H_2 = 1:2$ is obtained, which is the stoichiometric ratio for many typical fuel synthesis reactions (such as Fischer–Tropsch or methanol synthesis). The combined approach hence yields significant synergies and achieves

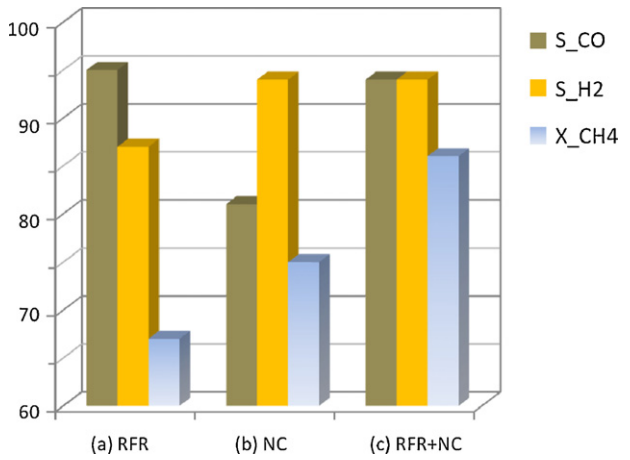

Fig. 10. Comparison between CO selectivity, H_2 selectivity, and CH_4 conversion in catalytic partial oxidation of a stoichiometric methane/air mixture utilizing (a) a conventional catalyst in a heat-integrated RFR (left group), (b) a Pt-BHA nanocatalyst ("NC") in a conventional steady-state reactor (center), and (c) combining the heat-integrated reactor with the nanostructured catalyst (right).

syngas yields in excess of 80% in a simple, compact, autothermal configuration operated with air feed.

4. Summary and conclusions

Process intensification is an exciting area of chemical and process engineering which is becoming increasingly important in the search for cleaner, more efficient, and more sustainable process design. The present contribution aimed specifically to draw attention to the opportunities of true multiscale process intensification in the field of catalytic fuel processing by reviewing results from the author's laboratory on catalytic partial oxidation of methane to synthesis gas (CPOM).

We demonstrated that heat-integrated reactors allow overcoming thermodynamic limitations typical for partial oxidation of hydrocarbons at autothermal conditions, and that "nano-engineered" catalysts complement the reactor concept by enabling the necessary catalyst stability as well as offering further increased catalyst activity. The combination of the integrated reactor concept with the nanostructured catalyst resulted not only in a "linear" superposition of the advantages of each PI principle (specifically the high CO selectivity of the RFR and the high H_2 selectivity of the nanocatalyst), but in a strong synergetic effect as reflected in increased methane conversion and improved CO:H_2 ratio. Such synergies are a characteristic element of successful multiscale process intensification and can form a guiding principle for the development of multiscale PI principles.

While the present discussion was limited to CPOM, similar results for oxidative dehydrogenation of ethane to ethylene, where kinetic rather than thermodynamic limitations have to be overcome [40], and for autothermal reforming of methane, where the application of the reverse-flow reactor concept results in a strongly expanded reactor operation range [58], demonstrate that heat-integration is not only beneficial for catalytic partial oxidation of methane, but that the presently discussed principles can be applied to a wide range of related catalytic fuel processing applications. Similarly, the importance of designing catalysts which enable to exploit the full potential of intensified reactor concepts is increasingly being acknowledged [59–61]. The presently discussed nanostructured materials have already found application in related processes, such as chemical looping combustion, an emerging clean combustion technology which shows many analogies to the technologies discussed here (such as a periodic process operation principle and the need for highly active and robust carrier materials) [52,53,62–64].

Overall, "process intensification" has come of age, as reflected, for example, in the dedication of an entire research journal to this topic [65]. At the same time, industrial implementation of process intensification is taking place at a rapid pace across a broad range of chemical industries, led by microreaction technology and reactive distillation processes [66–69]. By acknowledging the multiscale nature of catalytic processes and hence extending the conventional PI approach towards the "nanoscale" design of novel catalysts, PI is set to advance towards the next stage of development. This systematic pursuit of *multiscale* process intensification principles will be key for cleaner, more energy- and resource-efficient production of energy, fuels, and chemicals, in particular for small(er)-scale, decentralized processes with increased utilization of local resources.

References

[1] U.N.E. Programme, Climate in Peril, Birkeland Trykkeri, Norway, 2009.
[2] M. Alamaro, IEEE Technol. Soc. Mag. 13 (1994) 20.
[3] IEA, Cities, Towns, and Renewable Energy, 2009.
[4] C. Ramshaw, Chem. Eng. 416 (1985) 30.
[5] W. de Vries, European Roadmap for Process Intensification, http://www.senternovem.nl/mmfiles/Report%20%27European%20Roadmap%20for%20Process%20Intensification%27_tcm24-258503.pdf, 2007.
[6] M.V. Koch, K.M. VandenBussche, R.W. R.W. Chrisman (Eds.), Micro Instrumentation: For High Throughput Experimentation and Process Intensification, VCH-Wiley, Weinheim, 2007.
[7] N. Kockmann (Ed.), Micro Process Engineering, VCH-Wiley, Weinheim, 2006.
[8] Y. Wang, J.D. Holladay (Eds.), Microreactor Technology and Process Intensification, ACS Publishing, Washington, 2005.
[9] K.R. Westerterp, Chem. Eng. Sci. 47 (1992) 9.
[10] D.W. Agar, Chem. Eng. sci. 54 (1999) 1299.
[11] F.M. Dautzenberg, M. Mukherjee, Chem. Eng. Sci. 56 (2001) 251.
[12] K. Sundmacher, A. Kienle (Eds.), Reactive Distillation, Wiley-VCH, Weinheim, 2002.
[13] J.G. Sanchez Marcano, T.T. Tsotsis, Ullmann's Encyclopedia of Industrial Chemistry, vol. 21, Wiley-VCH Verlag, Weinheim, 2005, p. 223.
[14] H. Schmidt-Traub, A. Gorak (Eds.), Integrated Reaction and Separation Operations, Springer, Berlin, 2006.
[15] V.H. Agreda, L.R. Partin, W.H. Heise, Chem. Eng. Progr. 86 (1990) 40.
[16] K.V.K. Boodhoo, R.J. Jachuck, Green Chem. 2 (2000) 235.
[17] P. Oxley, C. Brechtelsbauer, F. Ricard, N. Lewis, C. Ramshaw, Ind. Eng. Chem. Res. 39 (2000) 2175.
[18] G. Eigenberger, in: G. Ertl, H. Közinger, J. Weitkamp (Eds.), Handbook of Heterogeneous Catalysis, vol. 4, 1997, p. 1399.
[19] G. Kolios, J. Frauhammer, G. Eigenberger, Chem. Eng. Sci. 55 (2000) 5945.
[20] A. Stankiewicz, J.A. Moulijn, Re-engineering the Chemical Processing Plant, Marcel Dekker, 2003.
[21] D. Reay, C. Ramshaw, A. Harve, Process Intensification: Engineering for Efficiency, Sustainability and Flexibility, Butterworth-Heinemann, 2008.
[22] F.J. Keil (Ed.), Modeling of Process Intensification, VCH-Wiley, Weinheim, 2007.
[23] I. Wender, Fuel Proc. Technol. 48 (1996) 189.
[24] J.R. Rostrup-Nielsen, Catal. Today 71 (2002) 243.
[25] D. Neumann, M. Kirchhoff, G. Veser, Catal. Today 98 (2004) 565.
[26] K. Aasberg-Petersen, J.H.B. Hansen, T.S. Christensen, I. Dybkjaer, P.S. Christensen, C.S. Nielsen, S. Madsen, J.R. Rostrup-Nielsen, Appl. Catal. A 221 (2001) 379.
[27] D.A. Hickman, E.A. Haupfear, L.D. Schmidt, Catal. Lett. 17 (1993) 223.
[28] L.D. Schmidt, M. Huff, S.S. Bharadwaj, Chem. Eng. Sci. 49 (1994) 3981.
[29] K. Heitnes, S. Lindeberg, O.A. Rokstad, A. Holmen, Catal. Today 24 (1995) 211.
[30] T.F. Liu, C. Snyder, G. Veser, Ind. Eng. Chem. Res. 46 (2007) 9045.
[31] R. Horn, K.A. Williams, N.J. Degenstein, L.D. Schmidt, Chem. Eng. Sci. 62 (2007) 1298.
[32] G. Veser, in: Y. Wang, J.D. Holladay (Eds.), Process Intensification and Microreaction Technology, vol. 914, ACS Symposium Series, New York, 2005, p. 145.
[33] U. Friedle, G. Veser, Chem. Eng. Sci. 54 (1999) 1325.
[34] G. Veser, J. Frauhammer, U. Friedle, Catal. Today 61 (2000) 55.
[35] G.K. Boreskov, Y.S. Matros, Appl. Catal. 5 (1983) 337.
[36] G. Eigenberger, U. Nieken, Chem. Eng. Sci. 43 (1988) 2109.
[37] Y. Matros, G. Bunimovich, Catal. Rev. Sci. Eng. 38 (1996) 1.
[38] D. Neumann, G. Veser, AIChE J. 51 (2005) 210.
[39] D. Neumann, V. Gepert, G. Veser, Ind. Eng. Chem. Res. 43 (2004) 4657.
[40] T. Liu, V. Gepert, G. Veser, Chem. Eng. Res. Des. 83 (2005) 611.
[41] C.H. Bartholomew, Appl. Catal. A 212 (2001) 17.
[42] A. Mitri, D. Neumann, T. Liu, G. Veser, Chem. Eng. Sci. 59 (2004) 5527.
[43] W.T. Liu, Chem. Eng. Sci. 62 (2007) 3502.
[44] A.T. Bell, Science 299 (2003) 1688.
[45] P.Z. Pawlov, Z. Phys. Chem. 65 (1909) 545.

[46] P. Buffat, J.-P. Borel, Phys. Rev. A 13 (1976) 2287.
[47] M. Kirchhoff, U. Specht, G. Veser, in: G. Emig (Ed.), Innovation in the Manufacture and Use of Hydrogen, DGMK Publishing, Hamburg, 2003, p. 33.
[48] M. Kirchhoff, U. Specht, G. Veser, Nanotechnology 16 (2005) S401.
[49] M.P. Pileni, Langmuir 13 (1997) 3266.
[50] S. Eriksson, U. Nylen, S. Rojas, M. Boutonnet, Appl. Catal. A 265 (2004) 207.
[51] T. Sanders, P. Papas, G. Veser, Chem. Eng. J. 142 (2008) 122.
[52] H.J. Tian, K. Chaudhari, T. Simonyi, J. Poston, T.F. Liu, T. Sanders, G. Veser, R. Siriwardane, Energy Fuels 22 (2008) 3744.
[53] R.D. Solunke, G. Veser, Energy Fuels 23 (2009) 4787.
[54] A. Cao, G. Veser, Nat. Mater. 9 (2010) 75.
[55] H. Arai, H. Fukuzawa, Catal. Today 26 (1995) 217.
[56] J. Schicks, D. Neumann, U. Specht, G. Veser, Catal. Today 83 (2003) 287.
[57] M. Kirchhoff, U. Specht, G. Veser, NSTI Nanotechnology 2004, Boston, 2004.
[58] T.F. Liu, H. Temur, G. Veser, Chem. Eng. Technol. 32 (2009) 1358.
[59] J.C. Charpentier, Comp. Chem. Eng. 33 (2009) 936.
[60] J.C. Charpentier, Chem. Eng. Res. Des. 88 (2010) 248.
[61] G.D. Stefanidis, D.G. Vlachos, Chem. Eng. Sci. 65 (2010) 398.
[62] M. Ishida, H. Jin, Energy Conv. Manag. 38 (1997) S187.
[63] M.M. Hossain, H. De Lasa, Chem. Eng. Sci. 63 (2008) 4433.
[64] R.D. Solunke, G. Veser, Ind. Eng. Chem. Res. (2010), in press.
[65] Chemical & Engineering Processing: Process Intensification (Elsevier).
[66] G.J. Harmsen, Chem. Eng. Proc. 46 (2007) 774.
[67] S. Becht, R. Franke, A. Geisselmann, H. Hahn, Chem. Eng. Proc. 48 (2009) 329.
[68] J. Harmsen, Chem. Eng. Proc. 49 (2010) 70.
[69] J.J. Lerou, A.L. Tonkovich, L. Silva, S. Perry, J. McDaniel, Chem. Eng. Sci. 65 (2010) 380.